
SGD and Weight Decay Provably Induce a Low-Rank Bias in Deep Neural Networks

Tomer Galanti

Center for Brains, Mind, and Machines
Massachusetts Institute of Technology
galanti@mit.edu

Zachary Siegel

Department of Computer Science
Princeton University
zss@princeton.edu

Aparna Gupte

MIT EECS
Massachusetts Institute of Technology
agupte@mit.edu

Tomaso Poggio

Center for Brains, Mind, and Machines
Massachusetts Institute of Technology
tp@csail.mit.edu

Abstract

We study the bias of Stochastic Gradient Descent (SGD) to learn low-rank weight matrices when training deep ReLU neural networks. Our results show that training neural networks with mini-batch SGD and weight decay causes a bias towards rank minimization over the weight matrices. Specifically, we show, both theoretically and empirically, that this bias is more pronounced when using smaller batch sizes, higher learning rates, or increased weight decay. Additionally, we predict and observe empirically that weight decay is necessary to achieve this bias. Unlike previous literature, our analysis does not rely on assumptions about the data, convergence, or optimality of the weight matrices and applies to a wide range of neural network architectures of any width or depth. Finally, we empirically investigate the connection between this bias and generalization, finding that it has a marginal effect on generalization.

1 Introduction

Stochastic gradient descent (SGD) is a widely used optimization technique for training deep learning models [1]. While it was initially developed to address the computational challenges of gradient descent, recent studies suggest that SGD also provides regularization that prevents overparameterized models from converging to minima that do not generalize well [2, 3, 4, 5]. For instance, empirical studies have shown that SGD outperforms gradient descent [5] and that smaller batch sizes result in better generalization [6, 4]. However, the full range of regularization effects induced by SGD is not yet fully understood.

One area of recent research focuses on characterizing the implicit regularization of gradient-based optimization and its relationship to generalization in deep learning. Several papers have examined the potential bias of gradient descent or stochastic gradient descent toward rank minimization. Empirically, it was shown [7, 8, 9, 10, 11] that replacing weight matrices with low-rank approximations results in only a small drop in accuracy, suggesting that the weight matrices at convergence may be close to low-rank matrices. Following this line of work, various attempts were made to understand the origins of this low-rank bias and its potential relation with generalization.

Initially, it was believed that the implicit regularization in matrix factorization could be characterized in terms of the nuclear norm of the corresponding linear predictor [12]. This conjecture was later refuted [13]. Subsequent conjecture posits that rank minimization may play a key role in explaining

Table 1: **The assumptions and results of various papers on low-rank bias in deep learning.** The last column shows the result of each paper. The notation Lin_L denotes a composition of L linear layers, and σ represents the ReLU activation. N/A is used when the paper does not specify a constraint. Our paper considers a much more realistic setting than all of the previous papers.

Paper	Architecture	Data	Objective function	Optimizer	Convergence	Result
[18]	Lin_L	Linearly separable	Exponential/logistic loss	GF	N/A	Each layer has rank ≤ 1
[20]	$\text{Lin}_1 \circ \sigma \circ \text{Lin}_1$	1-dimensional	Min L_2 regularization s.t. data fitting	N/A	Global optimum	First layer has rank ≤ 1
[16]	$\text{Lin}_1 \circ \sigma \circ \text{Lin}_L$	d -dimensional	Min L_2 regularization s.t. data fitting	N/A	Global optimum	Bottom linear transformation has rank $\leq d$
[19]	$\text{Lin}_K \circ \sigma \circ \text{Lin}_1 \circ \dots \circ \sigma \circ \text{Lin}_1$	Linearly separable	Exponential/logistic loss	GF	N/A	Top K layers have rank ≤ 1
[17]	$\text{Lin}_1 \circ \sigma \circ \text{Lin}_1 \circ \dots \circ \sigma \circ \text{Lin}_1$	Separable by a depth L' network	Min L_2 regularization s.t. fitting the data	N/A	Global optimum	Top $L - L'$ layers have rank ≤ 2
Ours	Res, Conv, Lin, Activation	N/A	Differentiable loss + L_2 regularization	SGD	N/A	Each layer has rank $\mathcal{O}(1)$ (w.r.t the width)

generalization in deep learning. For instance, [14] conjectured that the implicit regularization in matrix factorization can be explained by rank minimization, and also hypothesized that some notion of rank minimization may be key to explaining generalization in deep learning. Additionally, [13] established evidence that the implicit regularization in matrix factorization is a heuristic for rank minimization.

Several studies [15, 16, 17] have examined the rank of weight matrices in neural networks that globally minimize L_2 regularization while fitting training data. Specifically, [15] demonstrated that for data on a 1-dimensional manifold, the weight matrices of a two-layer network become rank-1 at the global minimum, a finding later extended in [16] to show that the weight matrix has rank $\leq d$ when the data lies on a d -dimensional space. Additionally, [17] discovered that for sufficiently deep ReLU networks to fit the data, the weight matrices at the top-most layers become low-rank at the global minimum.

Despite recent progress in characterizing low-rank weight matrices at the global minimum, the underlying reasons for the low-rank bias in optimization are still unclear. Previous research [18] has shown that gradient flow (GF) training of univariate linear networks with exponentially-tailed classification losses learns weight matrices of rank-1 when the data is linearly separable. In a more recent study [19], the authors extended this result and showed that when successfully training a ReLU network with multiple linear layers at the top using GF, the top layers converge to rank-1 weight matrices.

Contributions. In this paper, we show that using mini-batch Stochastic Gradient Descent (SGD) and weight decay *implicitly minimizes the rank* of the learned weight matrices during the training of neural networks, particularly encouraging the *learning of low-dimensional feature manifolds*. Within the active field that investigates these properties [21, 18, 20, 19, 17], our analysis is the first to characterize the low-rank bias in a realistic setting, without is the first to characterize how SGD and weight decay induce a low-rank bias in all of the weight matrices of a wide range of neural network architectures (e.g., with residual connections [22], self-attention layers [23], convolutional layers [24]), without making assumptions about the data (e.g., linear separability or low dimensionality) and convergence. Our theoretical analysis predicts that smaller batch sizes, higher learning rates, or increased weight decay results in a decrease in the rank of the learned matrices, and that weight decay is necessary to achieve this bias. The scope of the analysis is fairly general, covering deep Leaky ReLU networks trained with SGD for minimizing a differentiable loss function with L_2 regularization (i.e., weight decay). The neural networks may include fully-connected layers, residual connections, and convolutional layers. Our results are compared with the previous literature in Tab. 1.

In addition to our theoretical analysis, we provide a comprehensive empirical analysis in which we examine the regularization effects of different hyperparameters on the rank of weight matrices for various network architectures. Additionally, we carried out several experiments to examine the connection between low-rank bias and generalization. Our findings suggest that although low-rank bias is not crucial for good generalization, it is associated with a slight improvement in performance.

2 Problem Setup

We study the influence of using mini-batch SGD in conjunction with weight decay on the ranks of the learned weight matrices of neural networks in standard learning settings. Namely, we consider a parametric model $\mathcal{F} \subset \{f' : \mathcal{X} \rightarrow \mathbb{R}^q\}$, where each function $f_W \in \mathcal{F}$ is specified by a vector of parameters $W \in \mathbb{R}^N$. The goal is to learn a function from a training dataset $S = \{x_i\}_{i=1}^m$. For each sample we have a loss function measuring the performance on that sample $\ell_i : \mathbb{R}^q \rightarrow \mathbb{R}$ which is

simply a differentiable function. For example, in supervised learning we have $\ell_i(u, y_i)$, where y_i is the label of the i th sample. The model is trained to minimize the regularized empirical risk,

$$L_S^\lambda(f_W) := \frac{1}{m} \sum_{i=1}^m \ell_i(f_W(x_i)) + \lambda \|W\|_2^2,$$

where $\lambda > 0$ is a predefined hyperparameter and $\|\cdot\|_2$ is the Frobenius norm. To accomplish this task, we typically use mini-batch SGD, as outlined in the following paragraph.

Model architecture. In this paper, we consider a broad set of models, including but not limited to neural networks with fully-connected layers, residual connections, convolutional layers, pooling layers, sub-differentiable activation functions (e.g., sigmoid, tanh, ReLU, Leaky ReLU), self-attention layers and siamese layers. In this framework, the model $f_W(x) := h(x; W^1, \dots, W^k)$ is a function that takes a sequence of weight matrices W^1, \dots, W^k and an input vector x . Throughout the paper, we assume that for each layer $l \in [k]$, we can write $f_W(x) = g_l(W^l u_1^l(x, W_{|l}), \dots, W^l u_{m_l}^l(x, W_{|l}), W_{|l}, x)$, where g_l is a sub-differentiable function accepting vectors $W^l u_j^l(x, W_{|l})$, the parameters $W_{|l} = \{W^j\}_{j \neq l}$ and x as input. Here, $u_j^l(x, W_{|l})$ are functions of x and the weight matrices $W_{|l}$, viewed as a layer preceding W^l .

For example, a neural network with a fully-connected layer can be written as follows: $f_W(x) = g_l(W^l u^l(x, W_{|l}), W_{|l}, x)$, where $u^l(x, W_{|l})$ is the input to the fully-connected layer and $g_l(z, W_{|l}, x)$ takes the output $z = W^l u^l(x, W_{|l})$ of the fully-connected layer and returns the output of the neural network (e.g., by composing multiple layers on top of it). More specifically, a fully-connected network $f_W(x) = W^L \sigma(W^{L-1} \dots W^2 \sigma(W^1 x) \dots)$ can be written as $g_l(W^l u^l(x, W_{|l}))$, where $g_l(z) = W^L \sigma(W^{L-1} \dots W^{l+1} \sigma(z) \dots)$ and $u^l(x, W_{|l}) = \sigma(W^{l-1} \dots W^2 \sigma(W^1 x) \dots)$. We can also represent convolutional layers within this framework. We can think of a convolutional layer as a transformation that takes some input u and applies the same linear transformation to multiple ‘patches’ independently, $W^l u_1^l, \dots, W^l u_{m_l}^l$, where each u_j^l denotes a patch in the input u (a patch in this case is a subset of the coordinates in u), m_l is the number of patches and $W^l \in \mathbb{R}^{c_l \times c_{l-1} d_{l-1}}$ is a matrix representation of the kernel. In this case, $u^l(x, W_{|l})$ is the output of the layer below the convolutional layer and $u_j^l(x, W_{|l})$ is the j th patch that the convolutional layer is applied to. Furthermore, g_l is simple the composition of the layers following the given convolutional layer. In similar ways, we can also represent neural networks with residual connections, self-attention layers and pooling layers.

Optimization. We employ stochastic sub-gradient descent (SGD) to minimize the regularized empirical risk $L_S^\lambda(f_W)$ over a specified number of iterations T . We begin by initializing W_1 using a any initialization method. At each iteration t , we randomly select a batch $\tilde{S}_t \subset S$ of B samples, and update $W_{t+1} = W_t - \mu \nabla_W L_{\tilde{S}_t}^\lambda(f_{W_t})$, where $\mu > 0$ is the predefined learning rate and $\nabla_W g(W)$ represents a sub-gradient of $g: \mathbb{R}^n \rightarrow \mathbb{R}$. We use sub-gradient descent when dealing with models that are only sub-differentiable, such as ReLU neural networks (for more details, see section 14.2 in [25]). It is worth noting that when the model is differentiable, sub-gradient descent aligns with gradient descent.

3 Theoretical Results

In this section, we theoretically show that when training a neural network with SGD, the weight matrices tend to be close to matrices of a bounded rank. We begin by making a simple observation that the rank of $\nabla_{W^l} \ell(f_W(x))$ is bounded by m_l (see ‘Model architecture’ in Sec. 2) for any l and any sample x . Then, by recursively unrolling the optimization process, we express the weight matrix W_T^l as a sum of $(1 - \mu\lambda)^n W_{T-n}^l$ and nB gradients of the loss function with respect to W^l for different samples at different iterations. Since each one of these terms is a matrix of rank $\leq m_l$, we conclude that the distance between W_T^l and a matrix of rank $\leq m_l B n$ decays exponentially fast when increasing n .

Lemma 3.1. *Let ℓ be a differentiable loss function, f_W be a model as described in Sec. 2, let W^l be any weight matrix within f_W and let $x \in \mathbb{R}^d$ be any sample. Then, $\text{rank}(\nabla_{W^l} \ell(f_W(x))) \leq m_l$.*

Proof. Let $u_j = u_j^l(x, W_l)$ and $f_W(x)_r$ be the r th coordinate of $f_W(x)$. By the chain rule, we have the following identities $\nabla_{W^l} \ell(f_W(x)) = \sum_{r=1}^q \frac{\partial \ell(f_W(x))}{\partial f_W(x)_r} \cdot \frac{\partial f_W(x)_r}{\partial W^l}$ and $\frac{\partial f_W(x)_r}{\partial W^l} = \sum_{j=1}^{m_l} \frac{\partial f_W(x)_r}{\partial W^l u_j} \cdot \frac{\partial W^l u_j}{\partial W^l} = \sum_{j=1}^{m_l} \frac{\partial f_W(x)_r}{\partial W^l u_j} \cdot u_j^\top$. In particular, $\nabla_{W^l} \ell(f_W(x)) = \sum_{r=1}^q \frac{\partial \ell(f_W(x))}{\partial f_W(x)_r} \cdot \sum_{j=1}^{m_l} \frac{\partial f_W(x)_r}{\partial W^l u_j} \cdot u_j^\top = \sum_{j=1}^{m_l} \left(\sum_{r=1}^q \frac{\partial \ell(f_W(x))}{\partial f_W(x)_r} \cdot \frac{\partial f_W(x)_r}{\partial W^l u_j} \right) u_j^\top$ which is a sum of m_l outer products, hence, a matrix of rank $\leq m_l$. \square

The above lemma shows the rank of the gradient with respect to any weight matrix W^l is bounded by $\leq m_l$. In particular, for a fully-connected layer with weight matrix W^l , the sub-gradient of the loss function with respect to W^l is at most 1 and for a convolutional layer it is bounded by the number of patches upon which the kernel is being applied.

The following lemma provides an upper bound on the minimal distance between the network's weight matrices and matrices of bounded ranks.

Lemma 3.2. *Let $\|\cdot\|$ be any matrix norm and ℓ any differentiable loss function. Let f_W be a model as described in Sec. 2 and W^l be a weight matrix within f_W . Let $B \in [m]$. Then, for any $T > n$,*

$$\min_{\bar{W}^l: \text{rank}(\bar{W}^l) \leq m_l B n} \left\| \frac{W_T^l}{\|W_T^l\|} - \bar{W}^l \right\| \leq (1 - 2\mu\lambda)^n \cdot \frac{\|W_{T-n}^l\|}{\|W_T^l\|}.$$

Proof. Let $\tilde{S}_t \subset S$ the mini-batch that was used by SGD at iteration t . We have

$$\begin{aligned} W_T^l &= W_{T-1}^l - \mu \nabla_{W^l} L_{\tilde{S}_{T-1}}(f_{W_{T-1}}) - 2\mu\lambda W_{T-1}^l \\ &= (1 - 2\mu\lambda) W_{T-1}^l - \mu \nabla_{W^l} L_{\tilde{S}_{T-1}}(f_{W_{T-1}}). \end{aligned}$$

Similarly, we can write

$$W_{T-1}^l = (1 - 2\mu\lambda) W_{T-2}^l - \mu \nabla_{W^l} L_{\tilde{S}_{T-2}}(f_{W_{T-2}}).$$

This gives us

$$W_T^l = (1 - 2\mu\lambda)^2 W_{T-2}^l - \mu \nabla_{W^l} L_{\tilde{S}_{T-1}}(f_{W_{T-1}}) - \mu(1 - 2\mu\lambda) \nabla_{W^l} L_{\tilde{S}_{T-2}}(f_{W_{T-2}}).$$

By recursively applying this process n times, we have

$$\begin{aligned} W_T^l &= (1 - 2\mu\lambda)^n W_{T-n}^l - \mu \sum_{j=1}^n (1 - 2\mu\lambda)^{j-1} \nabla_{W^l} L_{\tilde{S}_{T-j}}(f_{W_{T-j}}) \\ &=: (1 - 2\mu\lambda)^n W_{T-n}^l + U_{T,n}^l. \end{aligned}$$

We notice that,

$$\nabla_{W^l} L_{\tilde{S}_{T-j}}(f_{W_{T-j}}) = \frac{1}{B} \sum_{x_i \in \tilde{S}_{T-j}} \nabla_{W^l} \ell_i(f_{W_{T-j}}(x_i)).$$

According to Lem. 3.1, we have $\text{rank}(\nabla_{W^l} \ell_i(f_{W_{T-j}}(x_i))) \leq m_l$. Therefore, $\text{rank}(\nabla_{W^l} L_{\tilde{S}_{T-j}}(f_{W_{T-j}})) \leq B m_l$ since $\nabla_{W^l} L_{\tilde{S}_{T-j}}(f_{W_{T-j}})$ is an average of B matrices of rank at most m_l . In particular, $\text{rank}(U_{T,n}^l) \leq m_l B n$ since $U_{T,n}^l$ is a sum of n matrices of rank at most $m_l B$. Therefore, we obtain that

$$\min_{\bar{W}^l: \text{rank}(\bar{W}^l) \leq m_l B n} \left\| W_T^l - \bar{W}^l \right\| \leq \left\| W_T^l - U_{T,n}^l \right\| = (1 - 2\mu\lambda)^n \|W_{T-n}^l\|.$$

Finally, by dividing both sides by $\|W_T^l\|$ we obtain the desired inequality. \square

The lemma above provides an upper bound on the minimal distance between the parameters matrix $W_T^{i,j}$ and a matrix of rank $\leq m_l B n$. The parameter t is a parameter of our choice that controls the looseness of the bound and is independent of the optimization process. The bound is proportional to $(1 - 2\mu\lambda)^n \frac{\|W_{T-n}^l\|}{\|W_T^l\|}$, which decreases exponentially with n as long as $\|W_T^l\|$ converges to a non-zero value. As a next step, we tune t to ensure that the bound would be smaller than ϵ . This result is summarized in the next theorem.

Theorem 3.3. Let $\|\cdot\|$ be any matrix norm and ℓ a differentiable loss function and $\mu, \lambda > 0$ such that $\mu\lambda < 0.5$, $B \in [m]$, $\epsilon > 0$ and $r = \frac{m_l B \log(2/\epsilon)}{2\mu\lambda}$. Let f_W be a model and W^l be a weight matrix within f_W . Assume that $\lim_{T \rightarrow \infty} (\|W_{T-1}^l\|/\|W_T^l\|) = 1$. Then, for sufficiently large T ,

$$\min_{\bar{W}^i: \text{rank}(\bar{W}^i) \leq r} \left\| \frac{W_T^l}{\|W_T^l\|} - \bar{W}^i \right\| \leq \epsilon.$$

Proof. We pick $n = \lceil \frac{\log(\epsilon/2)}{\log(1-2\mu\lambda)} \rceil$. Since n is independent of T , we have $\lim_{T \rightarrow \infty} \frac{\|W_{T-n}^l\|}{\|W_T^l\|} = \lim_{T \rightarrow \infty} \prod_{j=1}^n \frac{\|W_{T-j}^l\|}{\|W_{T-j+1}^l\|} = \prod_{j=1}^n \lim_{T \rightarrow \infty} \frac{\|W_{T-i}^l\|}{\|W_{T-i+1}^l\|} = 1$. Then, for any sufficiently large T , $\frac{\|W_{T-n}^l\|}{\|W_T^l\|} \leq 2$. We notice that for the selected T , we have $(1 - \mu\lambda)^n \leq \epsilon/2$. Hence, for any large T , we have, $(1 - \mu\lambda)^n \frac{\|W_{T-n}^l\|}{\|W_T^l\|} \leq \epsilon$. Furthermore, since $\mu\lambda < 0.5$, we also have $n \leq \frac{\log(2/\epsilon)}{2\mu\lambda}$ and $m_l B n \leq \frac{m_l B \log(2/\epsilon)}{2\mu\lambda}$. Therefore, by Lem. 3.2, we have the desired inequality. \square

The above theorem provides an upper bound on the rank of the learned weight matrices. It shows that when training the model, the normalized weight matrices $\frac{W_T^l}{\|W_T^l\|}$ become approximately matrices of rank at most $\frac{m_l B \log(2/\epsilon)}{2\mu\lambda}$. While $\frac{m_l B \log(2/\epsilon)}{2\mu\lambda}$ is not necessarily a small number, this bound is still non-trivial since $\frac{m_l B \log(2/\epsilon)}{2\mu\lambda} = \mathcal{O}(1)$ with respect to the iteration t and the size of the network (its width, depth, etc'). This result is particularly striking as it reveals a mechanism that encourages learning low-rank weight matrices that exclusively depends on the optimization process of SGD with weight decay, regardless of the weight initialization, geometric properties, or dimensionality of the data, which are largely irrelevant to the analysis. The assumption $\lim_{T \rightarrow \infty} (\|W_{T-1}^l\|/\|W_T^l\|) = 1$ generally occurs in practice and is validated in Appendix A. As a special case, it holds when $\|W_T^l\|$ converges to a non-zero value.

Predictions. Drawing from Thm. 3.3, we can make several predictions that can be tested empirically. Specifically, we anticipate that weight decay is necessary to achieve the low-rank bias. Moreover, using smaller batch sizes or increasing the weight decay or learning rate should result in SGD learning matrices of lower ranks. We empirically validate these predictions in Sec. 4.

4 Experiments

In this section, we empirically study how batch size, weight decay, and learning rate affect the rank of matrices in deep ReLU networks. We conduct separate experiments where we vary one hyperparameter while keeping the others constant to isolate its effect on the average rank. Additional experiments with a variety of architectures, datasets, as well as visualizations of the singular values of the weight matrices are provided in Appendix B. The plots are best viewed when zooming into the pictures. Each of the runs was done using a single GPU for at most 60 hours on a computing cluster with several available GPU types (e.g., GeForce RTX 2080, Tesla V-100).

4.1 Setup

Training and evaluation. In each experiment we trained ResNet-18 [22] instances for classification using Cross-Entropy loss minimization using SGD with batch size B , initial learning rate μ , 0 momentum, and weight decay λ . The models were trained with a decreasing learning rate of 0.1 at epochs 60, 100, and 200, and the training was stopped after 500 epochs. During training, we applied random cropping, random horizontal flips, and random rotations (by $15k$ degrees for k uniformly sampled from [24]) and standardized the data.

To study the influence of different hyperparameters on the rank of the weight matrices, in each experiment, we trained the models while varying one hyperparameter at a time, while keeping other hyperparameters constant. After each epoch, we compute the average rank across the network's weight matrices and its train and test accuracy rates. For a convolutional layer we represent its kernel parameters as a matrix, whose rows are vectorized versions of its kernels. To estimate the rank of

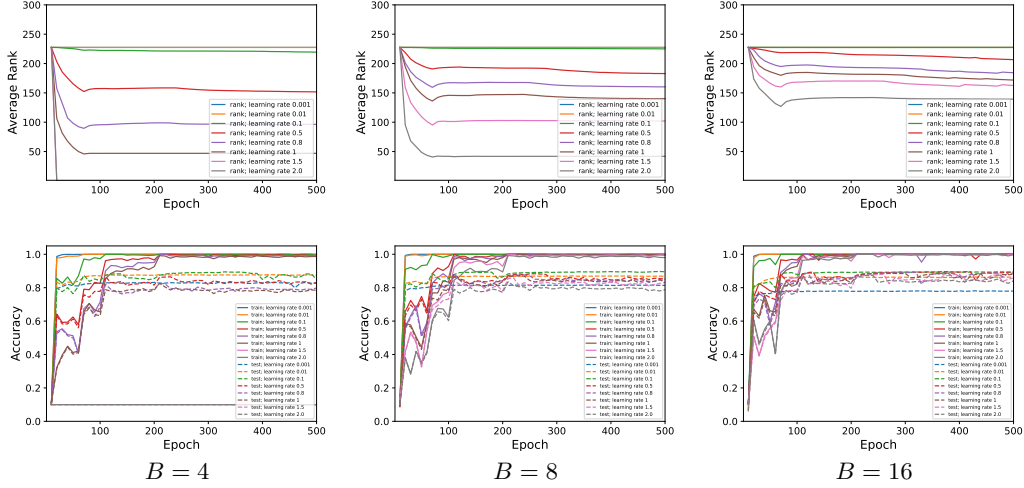


Figure 1: Average ranks and accuracy rates of ResNet-18 trained on CIFAR10 when varying μ . The top row shows the average rank across layers, while the bottom row shows the train and test accuracy rates for each setting. In this experiment, $\lambda = 5e-4$ and $\delta = 1e-3$.

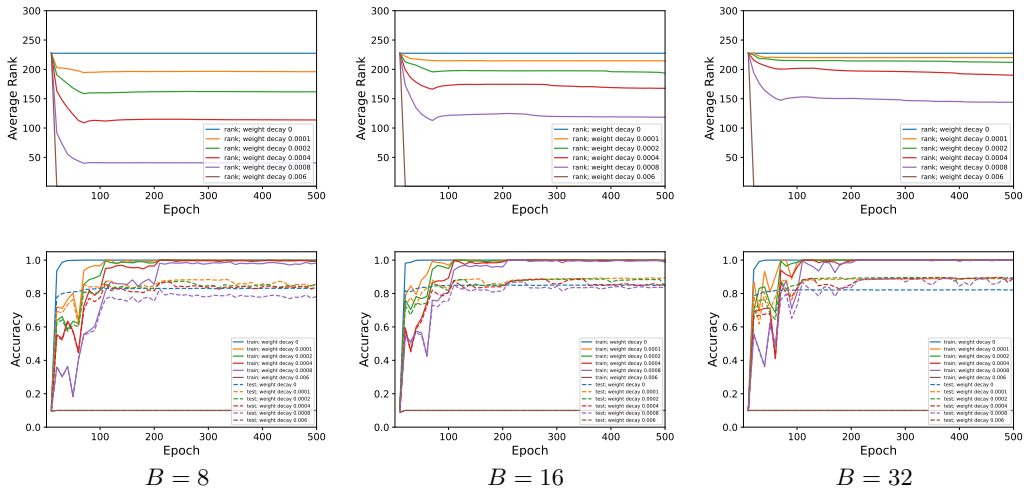


Figure 2: Average ranks and accuracy rates of ResNet-18 trained on CIFAR10 when varying λ . In this experiment, $\mu = 1.5$ and $\delta = 1e-3$.

a given matrix M , we count how many of the singular values of $\frac{M}{\|M\|_2}$ are out of the range $[-\delta, \delta]$, where δ is a small tolerance value (we used $\delta = 1e-3$ by default).

4.2 Results

Low-rank bias and hyperparameters. As shown in Figs. 1-4, decreasing the batch size, increasing the learning rate or the degree of weight decay strengthens the low-rank constraint on the network’s matrices, resulting in matrices of lower ranks. Furthermore, it is evident in Fig. 2 that the effect of batch size on the ranks of the weight matrices appears to be minimal when $\lambda = 0$, which suggests that weight decay is essential for imposing a noticeable low-rank bias on the weight matrices. These results align with the predictions made in Sec. 3.

Low-rank bias and generalization. We investigated the relationship between low-rank bias and generalization by training ResNet-18 models on CIFAR10 with varying batch sizes, while keeping λ and μ constant. To provide a fair comparison, we selected λ and μ to ensure all models perfectly fit

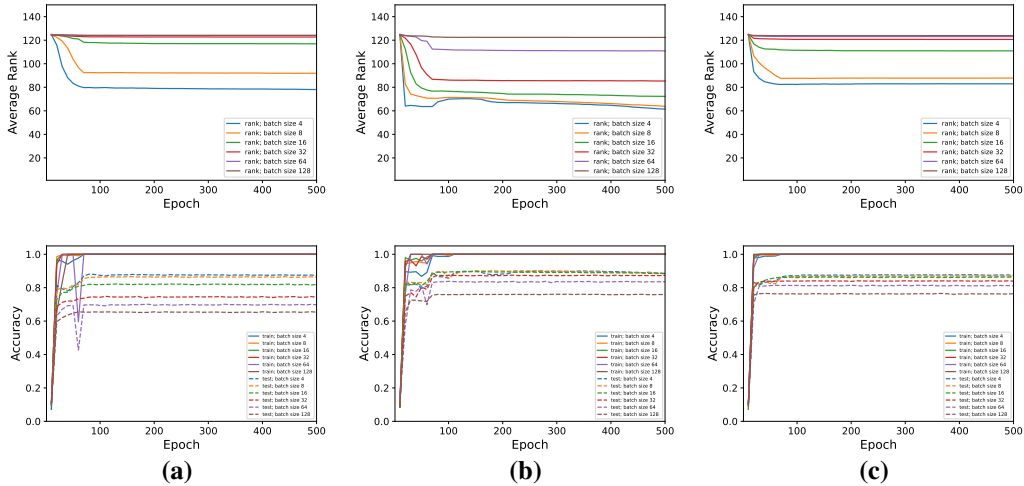


Figure 3: Average ranks and accuracy rates of ResNet-18 trained on CIFAR10 when varying B . In (a) we used $\mu = 1e-3$ and $\lambda = 6e-3$, in (b) we used $\mu = 5e-3$ and $\lambda = 6e-3$, and in (c) we used $\mu = 1e-2$ and $\lambda = 4e-4$. We used a threshold of $\delta = 1e-3$.

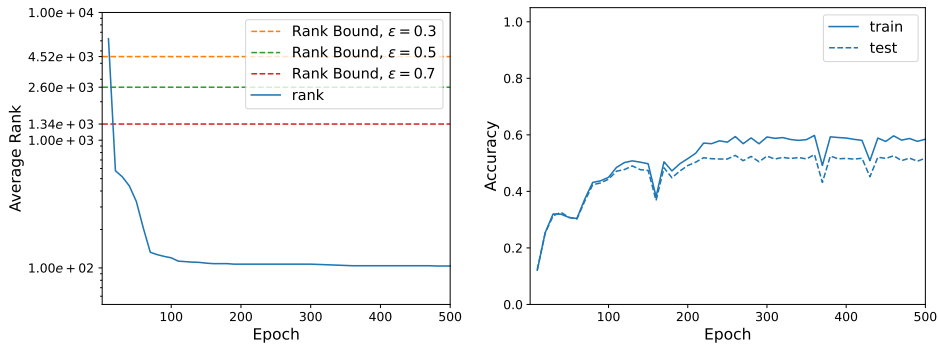


Figure 4: Comparing our bound with the averaged rank. We trained a MLP-BN-2-10000 on CIFAR10 with $B = 6$, $\mu = 0.1$, $\lambda = 8e-3$. We plot our bound for different choices of ϵ .

the training data. Our results, shown in Fig. 4, indicate that models trained with smaller batch sizes (i.e. lower rank in their weights) tend to generalize better as the test accuracy rate monotonically increases as the batch size decreases. Based on these findings, we hypothesize that when altering a certain hyperparameter, a neural network with a lower average rank will have better test performance than a network with the same architecture but higher rank matrices, assuming both networks perfectly fit the training data. For a similar experiment with VGG-16 [26] see the appendix.

Comparing our bound with the averaged rank. As mentioned above, our bound $m_l B \log(2/\epsilon)/(2\mu\lambda)$ is generally loose, but not trivial, as it scales as $\mathcal{O}(1)$ relative to the actual dimensions of the weight matrices. To demonstrate that our bound is non-trivial for wide neural networks, we trained an MLP-BN-2-10000 on CIFAR10 using $B = 6$, $\mu = 0.1$, and $\lambda = 8e-3$. As shown in Figure 4, the network is able to train (achieves a non-trivial training accuracy), and at the same time, the bound is strictly smaller than the width of 10000 for any $\epsilon \geq 0.3$.

5 Conclusions

Mathematically characterizing the inductive biases associated with SGD-trained neural networks is regarded as a significant open problem in the theory of deep learning [27]. In addition to its independent interest, a low-rank bias – though probably not necessary for generalization – may be a

key ingredient in an eventual characterization of the representation learning in deep networks. In fact, our preliminary experiments (see Fig. 4) suggest that this bias contributes to generalization.

In this work, we tackled one of the main inductive biases that were observed in empirical studies. Our study of deep neural networks trained with SGD provides a new way of thinking about weight decay. We show that SGD with weight decay forgets past updates exponentially fast, resulting in learned weights that are a mixture of recent training updates. As we show, this leads to a rank minimization mechanism, mainly controlled by the batch size, learning rate, and weight decay, regardless of the geometry of training data or dimensionality. An interesting follow-up question is whether this analysis can be extended to validate other empirical phenomena, such as implicitly induced sparsity [28], Grokking [29] and Neural Collapse at intermediate layers [30, 31].

Acknowledgements

We thank Andrea Pinto, Liane Galanti, Akshay Rangamani, Brian Cheung, Qianli Liao, Mengjia Xu, Ilja Kuzborskij, Mikhail Belkin, Eran Malach, X.Y. Han and Vardan Papyan for illuminating discussions during the preparation of this manuscript. This material is based upon work supported by the Center for Minds, Brains and Machines (CBMM), funded by NSF STC award CCF-1231216. This research was also sponsored by grants from the National Science Foundation (NSF-0640097, NSF-0827427) and Lockheed Martin Space Advanced Technology Center.

References

- [1] Léon Bottou. Stochastic gradient learning in neural networks. In *Proceedings of Neuro-Nîmes 91*, Nîmes, France, 1991. EC2.
- [2] Chiyuan Zhang, Samy Bengio, Moritz Hardt, Benjamin Recht, and Oriol Vinyals. Understanding deep learning requires rethinking generalization. *CoRR*, abs/1611.03530, 2016.
- [3] Stanislaw Jastrzebski, Zachary Kenton, Devansh Arpit, Nicolas Ballas, Asja Fischer, Yoshua Bengio, and Amos Storkey. Three factors influencing minima in sgd, 2017.
- [4] Nitish Shirish Keskar, Dheevatsa Mudigere, Jorge Nocedal, Mikhail Smelyanskiy, and Ping Tak Peter Tang. On large-batch training for deep learning: Generalization gap and sharp minima. In *International Conference on Learning Representations (ICLR)*, 2017.
- [5] Zhanxing Zhu, Jingfeng Wu, Bing Yu, Lei Wu, and Jinwen Ma. The anisotropic noise in stochastic gradient descent: Its behavior of escaping from sharp minima and regularization effects. In *Proceedings of the 36th International Conference on Machine Learning*, volume 139 of *Proceedings of Machine Learning Research*. PMLR, 2019.
- [6] Elad Hoffer, Itay Hubara, and Daniel Soudry. Train longer, generalize better: closing the generalization gap in large batch training of neural networks. In I. Guyon, U. Von Luxburg, S. Bengio, H. Wallach, R. Fergus, S. Vishwanathan, and R. Garnett, editors, *Advances in Neural Information Processing Systems*, volume 30. Curran Associates, Inc., 2017.
- [7] Emily L Denton, Wojciech Zaremba, Joan Bruna, Yann LeCun, and Rob Fergus. Exploiting linear structure within convolutional networks for efficient evaluation. In Z. Ghahramani, M. Welling, C. Cortes, N. Lawrence, and K.Q. Weinberger, editors, *Advances in Neural Information Processing Systems*, volume 27. Curran Associates, Inc., 2014.
- [8] Jose M. Alvarez and Mathieu Salzmann. Compression-aware training of deep networks. In *Proceedings of the 31st International Conference on Neural Information Processing Systems, NIPS'17*, page 856–867, Red Hook, NY, USA, 2017. Curran Associates Inc.
- [9] Murad Tukan, Alaa Maalouf, Matan Weksler, and Dan Feldman. No fine-tuning, no cry: Robust svd for compressing deep networks. *Sensors*, 21(16), 2021.
- [10] Xiyu Yu, Tongliang Liu, Xinchao Wang, and Dacheng Tao. On compressing deep models by low rank and sparse decomposition. In *2017 IEEE Conference on Computer Vision and Pattern Recognition (CVPR)*, pages 67–76, 2017.
- [11] Sanjeev Arora, Rong Ge, Behnam Neyshabur, and Yi Zhang. Stronger generalization bounds for deep nets via a compression approach. In Jennifer Dy and Andreas Krause, editors, *Proceedings of the 35th International Conference on Machine Learning*, volume 80 of *Proceedings of Machine Learning Research*, pages 254–263. PMLR, 10–15 Jul 2018.
- [12] Suriya Gunasekar, Blake Woodworth, Srinadh Bhojanapalli, Behnam Neyshabur, and Nathan Srebro. Implicit regularization in matrix factorization, 2017.
- [13] Zhiyuan Li, Yuping Luo, and Kaifeng Lyu. Towards resolving the implicit bias of gradient descent for matrix factorization: Greedy low-rank learning. *CoRR*, abs/2012.09839, 2020.
- [14] Noam Razin and Nadav Cohen. Implicit regularization in deep learning may not be explainable by norms. *CoRR*, abs/2005.06398, 2020.
- [15] Tolga Ergen and Mert Pilanci. Revealing the structure of deep neural networks via convex duality. *arXiv preprint arXiv:2002.09773*, 2020.
- [16] Greg Ongie and Rebecca Willett. The role of linear layers in nonlinear interpolating networks, 2022.
- [17] Nadav Timor, Gal Vardi, and Ohad Shamir. Implicit regularization towards rank minimization in relu networks. *CoRR*, abs/2201.12760, 2022.

- [18] Ziwei Ji and Matus Telgarsky. Directional convergence and alignment in deep learning. *CoRR*, abs/2006.06657, 2020.
- [19] Thien Le and Stefanie Jegelka. Training invariances and the low-rank phenomenon: beyond linear networks. In *International Conference on Learning Representations*, 2022.
- [20] Tolga Ergen and Mert Pilanci. Revealing the structure of deep neural networks via convex duality. In Marina Meila and Tong Zhang, editors, *Proceedings of the 38th International Conference on Machine Learning*, volume 139 of *Proceedings of Machine Learning Research*, pages 3004–3014. PMLR, 18–24 Jul 2021.
- [21] Sanjeev Arora, Nadav Cohen, Wei Hu, and Yuping Luo. Implicit regularization in deep matrix factorization. In *Proceedings of the 33rd International Conference on Neural Information Processing Systems*, Red Hook, NY, USA, 2019. Curran Associates Inc.
- [22] Kaiming He, Xiangyu Zhang, Shaoqing Ren, and Jian Sun. Deep residual learning for image recognition. In *2016 IEEE Conference on Computer Vision and Pattern Recognition (CVPR)*, pages 770–778, 2016.
- [23] Ashish Vaswani, Noam Shazeer, Niki Parmar, Jakob Uszkoreit, Llion Jones, Aidan N Gomez, Łukasz Kaiser, and Illia Polosukhin. Attention is all you need. In *Advances in Neural Information Processing Systems*, volume 30. Curran Associates, Inc., 2017.
- [24] Y. Lecun, L. Bottou, Y. Bengio, and P. Haffner. Gradient-based learning applied to document recognition. *Proceedings of the IEEE*, 86(11):2278–2324, 1998.
- [25] Shai Shalev-Shwartz and Shai Ben-David. *Understanding Machine Learning: From Theory to Algorithms*. Cambridge University Press, USA, 2014.
- [26] Karen Simonyan and Andrew Zisserman. Very deep convolutional networks for large-scale image recognition. *CoRR*, abs/1409.1556, 2014.
- [27] Behnam Neyshabur, Srinadh Bhojanapalli, David Mcallester, and Nati Srebro. Exploring generalization in deep learning. In I. Guyon, U. Von Luxburg, S. Bengio, H. Wallach, R. Fergus, S. Vishwanathan, and R. Garnett, editors, *Advances in Neural Information Processing Systems*, volume 30. Curran Associates, Inc., 2017.
- [28] Jonathan Frankle and Michael Carbin. The lottery ticket hypothesis: Finding sparse, trainable neural networks. In *International Conference on Learning Representations*, 2019.
- [29] Alethea Power, Yuri Burda, Harri Edwards, Igor Babuschkin, and Vedant Misra. Grokking: Generalization beyond overfitting on small algorithmic datasets, 2022.
- [30] Vardan Pappayan, X. Y. Han, and David L. Donoho. Prevalence of neural collapse during the terminal phase of deep learning training. *Proceedings of the National Academy of Sciences*, 117(40):24652–24663, 2020.
- [31] Tomer Galanti, Liane Galanti, and Ido Ben-Shaul. Comparative generalization bounds for deep neural networks. *Transactions on Machine Learning Research*, 2023.
- [32] Alexey Dosovitskiy, Lucas Beyer, Alexander Kolesnikov, Dirk Weissenborn, Xiaohua Zhai, Thomas Unterthiner, Mostafa Dehghani, Matthias Minderer, Georg Heigold, Sylvain Gelly, et al. An image is worth 16x16 words: Transformers for image recognition at scale. *arXiv preprint arXiv:2010.11929*, 2020.

A Additional Experiments

We performed additional experiments with different learning settings, including training on various datasets and using different architectures, to provide additional evidence of the bias toward rank minimization of SGD with weight decay. The experimental setting and the results are described below.

A.1 Experimental Details

Architectures. We consider five types of network architectures. (i) The first architecture is a multi-layer perceptron (MLP), denoted as MLP-BN- L - H , which comprises L hidden layers, each containing a fully-connected layer with width H , followed by batch normalization and ReLU activations. This architecture ends with a fully-connected output layer. (ii) The second architecture, referred to as RES-BN- L - H , consists of a linear layer with width H , followed by L residual blocks, and ending with a fully-connected layer. Each block performs a computation of the form $z + \sigma(n_2(W_2\sigma(n_1(W_1z))))$, where $W_1, W_2 \in \mathbb{R}^{H \times H}$, n_1, n_2 are batch normalization layers, and σ is the ReLU function. (iii) The third architecture is the convolutional network (VGG-16) proposed by [26], with dropout replaced by batch normalization layers to improve training performance, and a single fully-connected layer at the end. (iv) The fourth architecture is the residual network (ResNet-18) proposed in [22]. (v) The fifth architecture is a small visual transformer (ViT) [32]. We used a standard ViT that splits the input images into patches of size 4×4 , and includes 8 self-attention heads, each composed of 6 self-attention layers. The self-attention layers are followed by two fully-connected layers with a dropout probability of 0.1, and a GELU activation in between them.

Training and evaluation. We trained each model for classification using Cross-Entropy loss minimization between its logits and the one-hot encodings of the labels. The training was carried out by SGD with batch size B , initial learning rate μ , and weight decay λ . The MLP-BN- L - H , RES-BN- L - H , ResNet-18, and VGG-16 models were trained with a decreasing learning rate of 0.1 at epochs 60, 100, and 200, and the training was stopped after 500 epochs. The ViT models were trained using SGD with a learning rate that was decreased by a factor of 0.2 at epochs 60 and 100 and training was stopped after 200 epochs. During training, we applied random cropping, random horizontal flips, and random rotations (by $15k$ degrees for k uniformly sampled from [24]) and standardized the data.

A.2 Results

Training with different architectures. In the main text, we validated our predictions using the ResNet-18 architecture. For a more robust analysis, we conducted similar experiments with other architectures. Similar to the results in the main text, Figs. 5-13 show that, as we increase weight decay or learning rate or decrease batch size, the rank of the learned weight matrices tends to decrease. Additionally, when $\lambda = 0$, the influence of batch size or learning rate on the rank of the weight matrices is minimal, as seen in Figs. 5, 6, and 10.

Training with momentum. To ensure that our observations are applicable across diverse settings and not confined to a single optimization process, we conducted an additional experiment. In this experiment, we validated our observations by training a model using Stochastic Gradient Descent (SGD), weight decay, and momentum. Fig. 5 demonstrates that our predictions regarding the regularization effects of hyperparameters remain valid even when training the model with momentum.

Training on different datasets. In Fig. 13, we trained ResNet-18 instances on the MNIST and SVHN datasets, varying the learning rate while keeping the batch size ($B = 16$) and weight decay ($\lambda = 5e-4$) constant. The observed behavior, previously noted for CIFAR-10, is also replicated across these different datasets.

Verifying that $\lim_{T \rightarrow \infty} (\|W_{T-1}^l\|/\|W_T^l\|) = 1$. In Thm. 3.4 (main text) we made the assumption that $\lim_{T \rightarrow \infty} (\|W_{T-1}^l\|/\|W_T^l\|) = 1$. In order to validate this assumption, we trained various models and monitored the ratio between the norms of each layer at consecutive epochs. In each plot at Figs. 14-15 we report the ratios across different layers for a neural network with a certain learning rate. As can be seen, the ratios consistently converge to 1 during training.

Singular values. In our previous experiments, we measured the average rank of the weight matrices across different layers. To further investigate the rank of the learned weight matrices, we created

visualizations displaying the singular values of the weight matrices for each layer as a function of batch size.

For instance, in Figs. 16-17 we plotted the singular values of various layers for models that were trained in the setting of Fig. 3(b) (main text) and Fig. 12(c). Our results indicate that as a general tendency the singular values of each layer can be partitioned into two distinct groups: “small” singular values and “large” singular values (see the intersection point of all curves in the plots). Interestingly, the number of “small” singular values and “large” singular values is generally independent of the batch size. Moreover, “large” singular values decrease with the batch size and the “small” singular values increase with the batch size. This behavior provides additional evidence that when training with smaller batch sizes, the matrices have fewer large singular values compared to training with larger batch sizes.

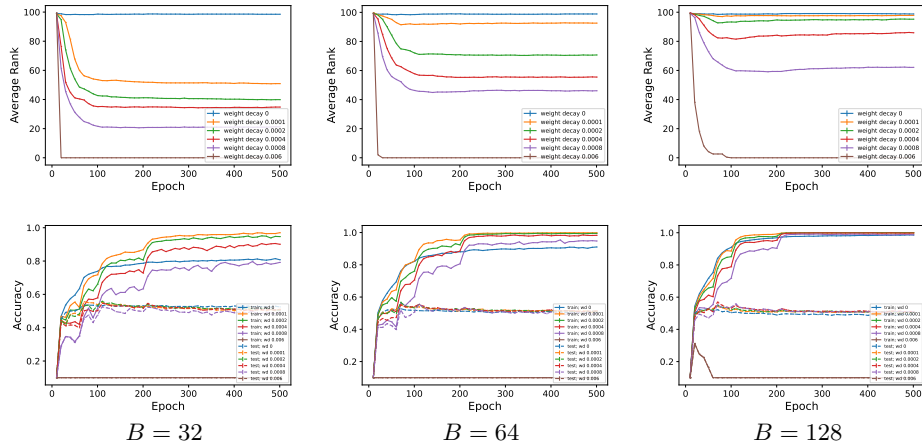


Figure 5: Average rank of MLP-BN-10-100 trained on CIFAR10 when varying λ . In this experiment, $\mu = 0.1$, momentum 0.9 and $\delta = 1e-3$.

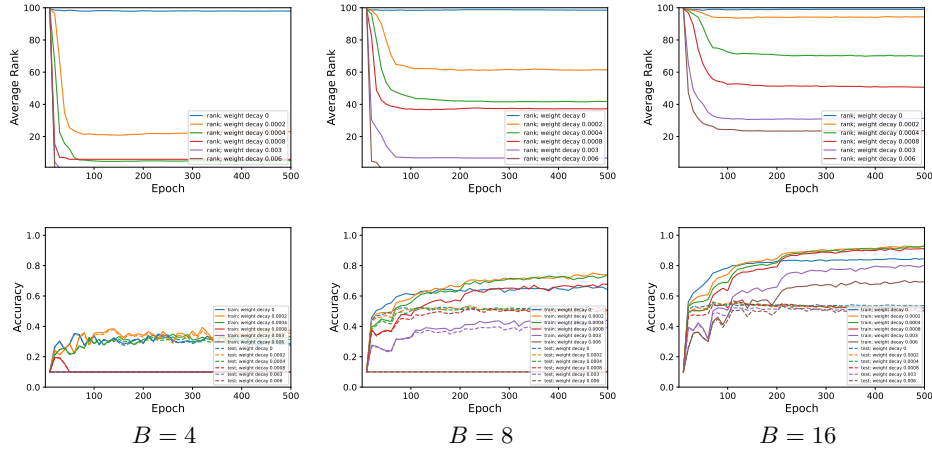


Figure 6: Average ranks and accuracy rates of MLP-BN-10-100 trained on CIFAR10 when varying λ . In this experiment, $\mu = 0.1$ and $\delta = 1e-3$.

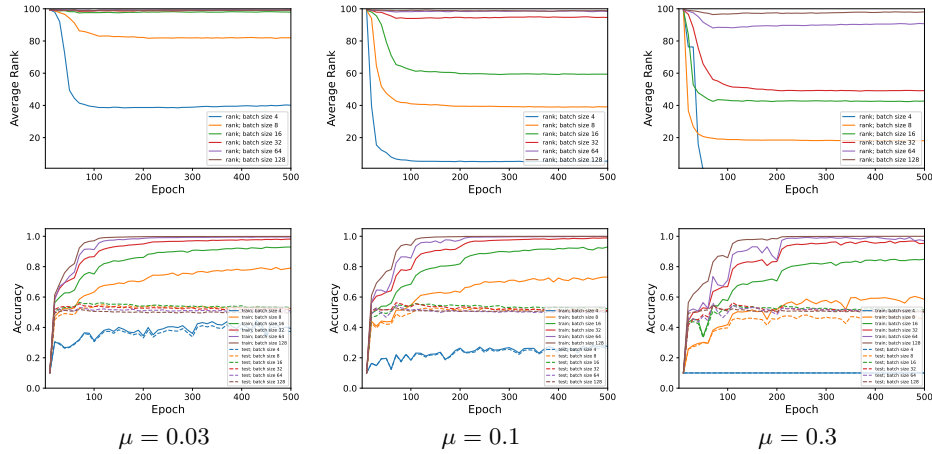


Figure 7: Average ranks and accuracy rates of MLP-BN-10-100 trained on CIFAR10 when varying B . In this experiment, $\lambda = 5e-4$ and $\delta = 1e-3$.

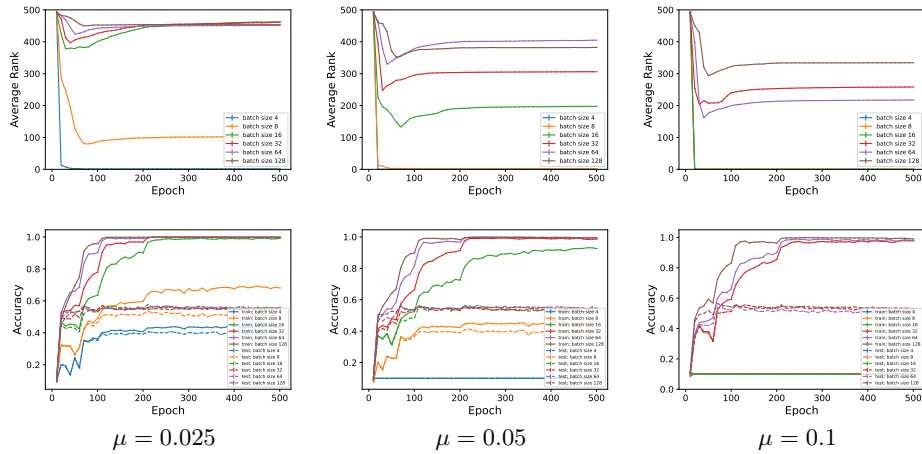


Figure 8: Average rank of RES-BN-5-500 trained on CIFAR10 when varying B . In this experiment, $\lambda = 5e-4$ and $\delta = 1e-3$.

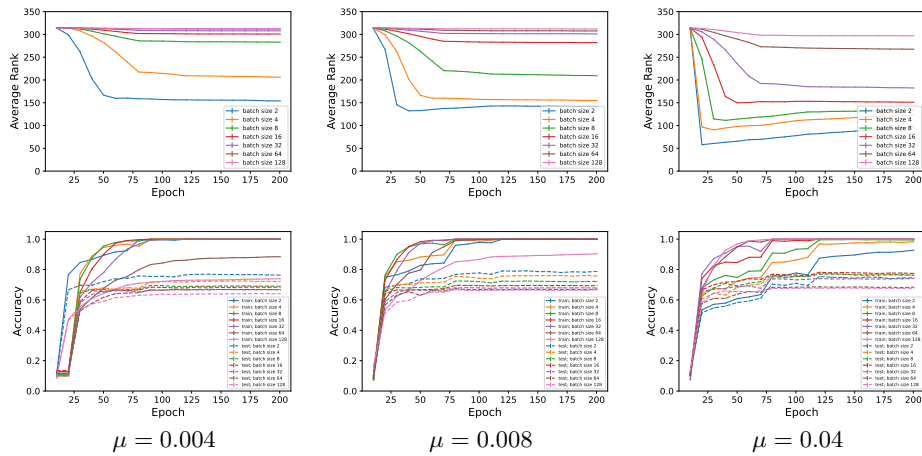


Figure 9: Average ranks and accuracy rates of ViT trained on CIFAR10 when varying B . In this experiment, $\lambda = 5e-4$ and $\delta = 1e-3$.

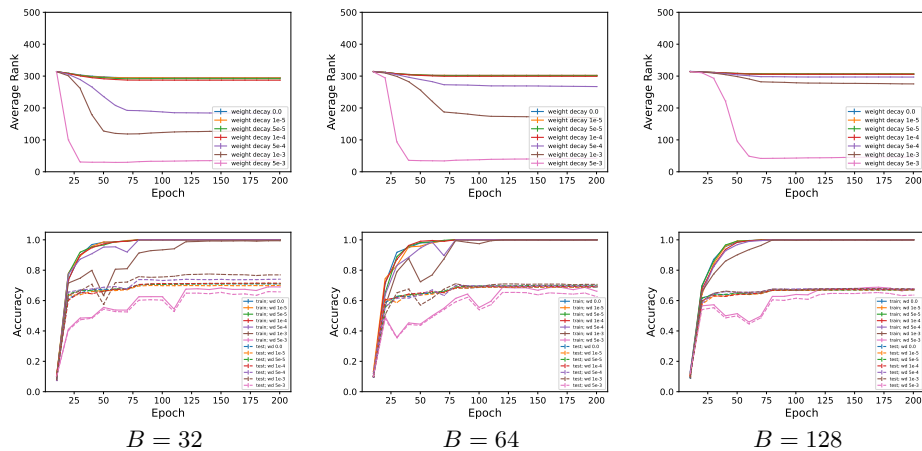


Figure 10: Average ranks and accuracy rates of ViT trained on CIFAR10 when varying λ . In this experiment, $\mu = 4e-2$ and $\delta = 1e-3$.

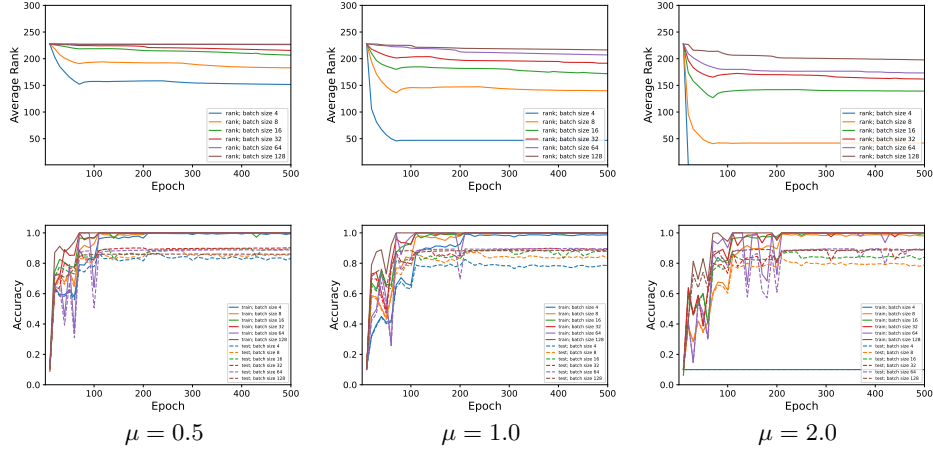


Figure 11: Average ranks and accuracy rates of ResNet-18 trained on CIFAR10 when varying B . In this experiment, $\lambda = 5e-4$ and $\delta = 1e-3$.

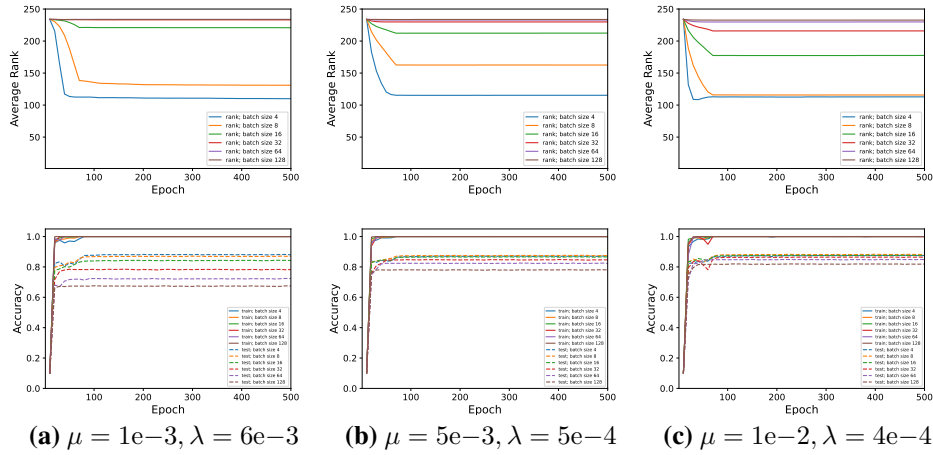


Figure 12: Average ranks and accuracy rates of VGG-16 trained on CIFAR10 when varying B . We used a threshold of $\delta = 4e-2$.

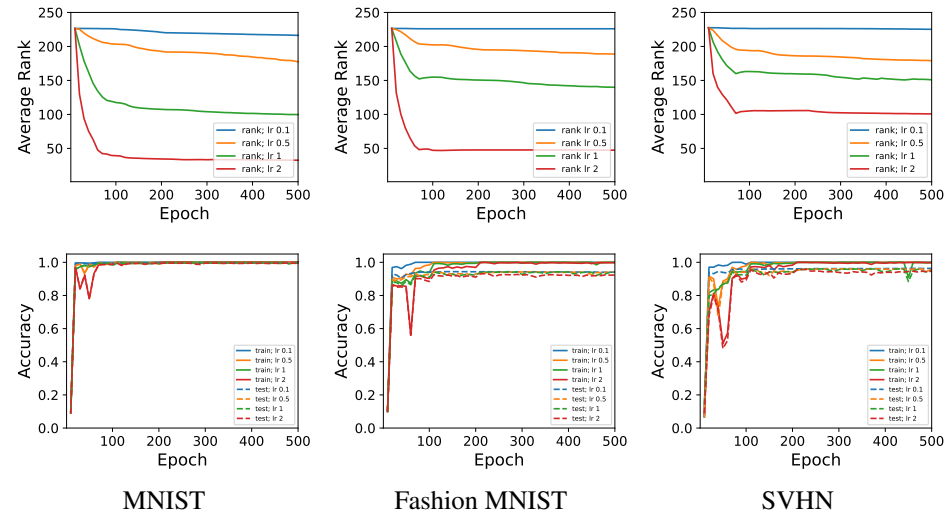


Figure 13: Average ranks and accuracy rates of ResNet-18 trained on MNIST, Fashion MNIST, and SVHN when varying μ . In this experiment, $B = 16$, $\lambda = 5e-4$ and $\delta = 1e-3$.

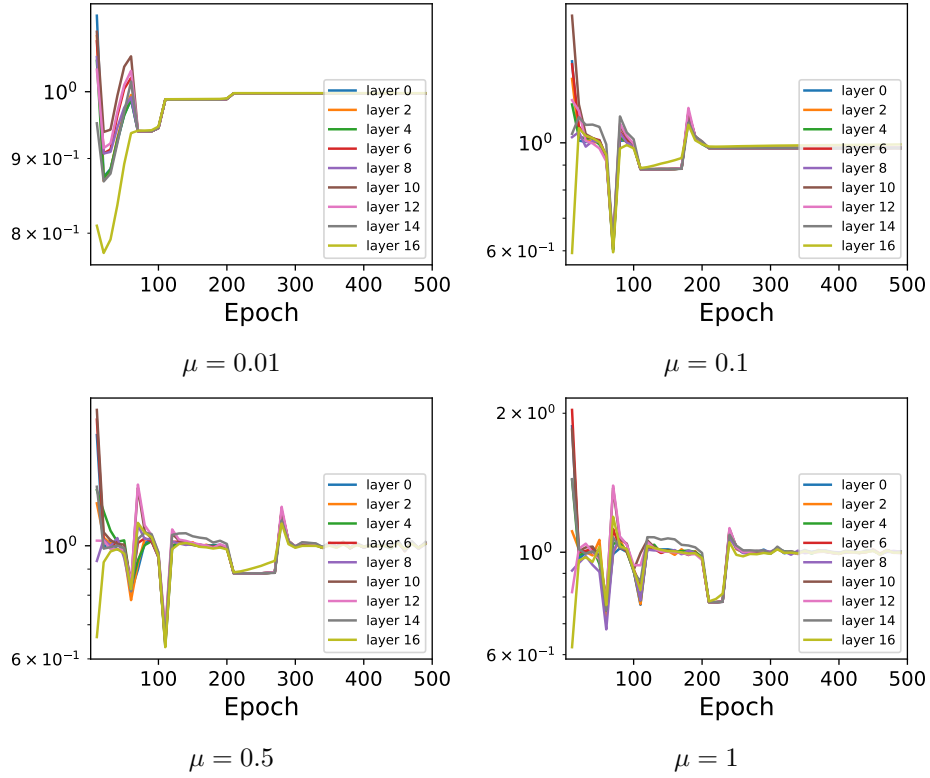


Figure 14: **Convergence of the weights for ResNet-18 trained on CIFAR10.** In this experiment, $B = 8$, $\lambda = 5e-4$ and $\delta = 0.01$ (see Fig. 1(mid) in the main text for the weight ranks and accuracy rates).

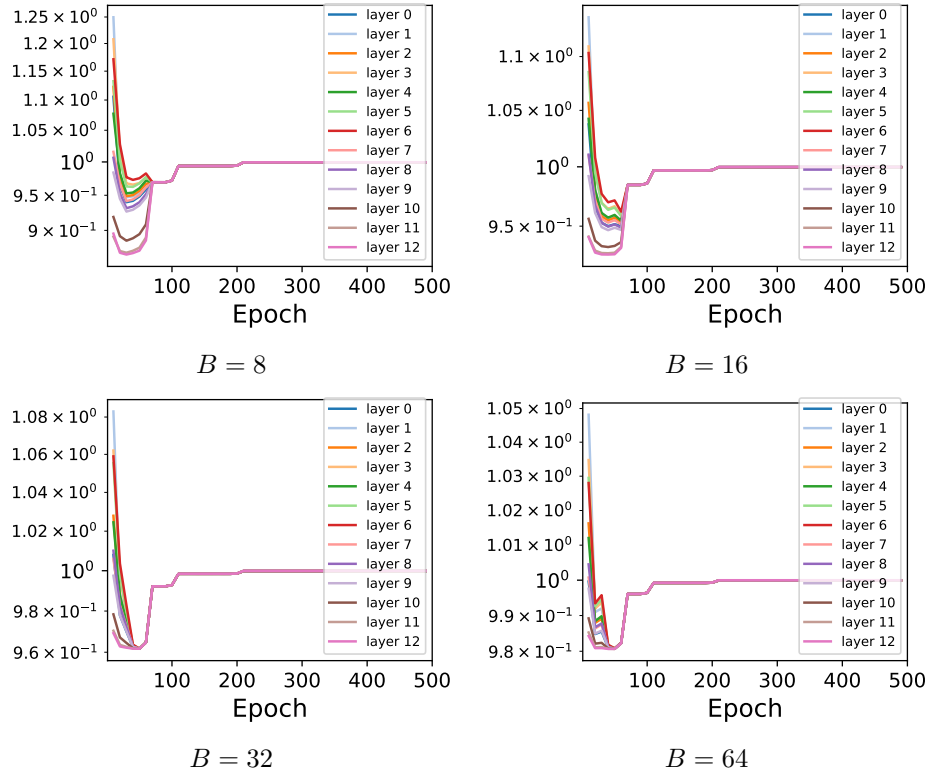


Figure 15: **Convergence of the weights for VGG-16 trained on CIFAR10.** In this experiment, $\mu = 5e-3$, $\lambda = 5e-4$ and $\delta = 0.01$ (see Fig. 12(b) for the weight ranks and accuracy rates).

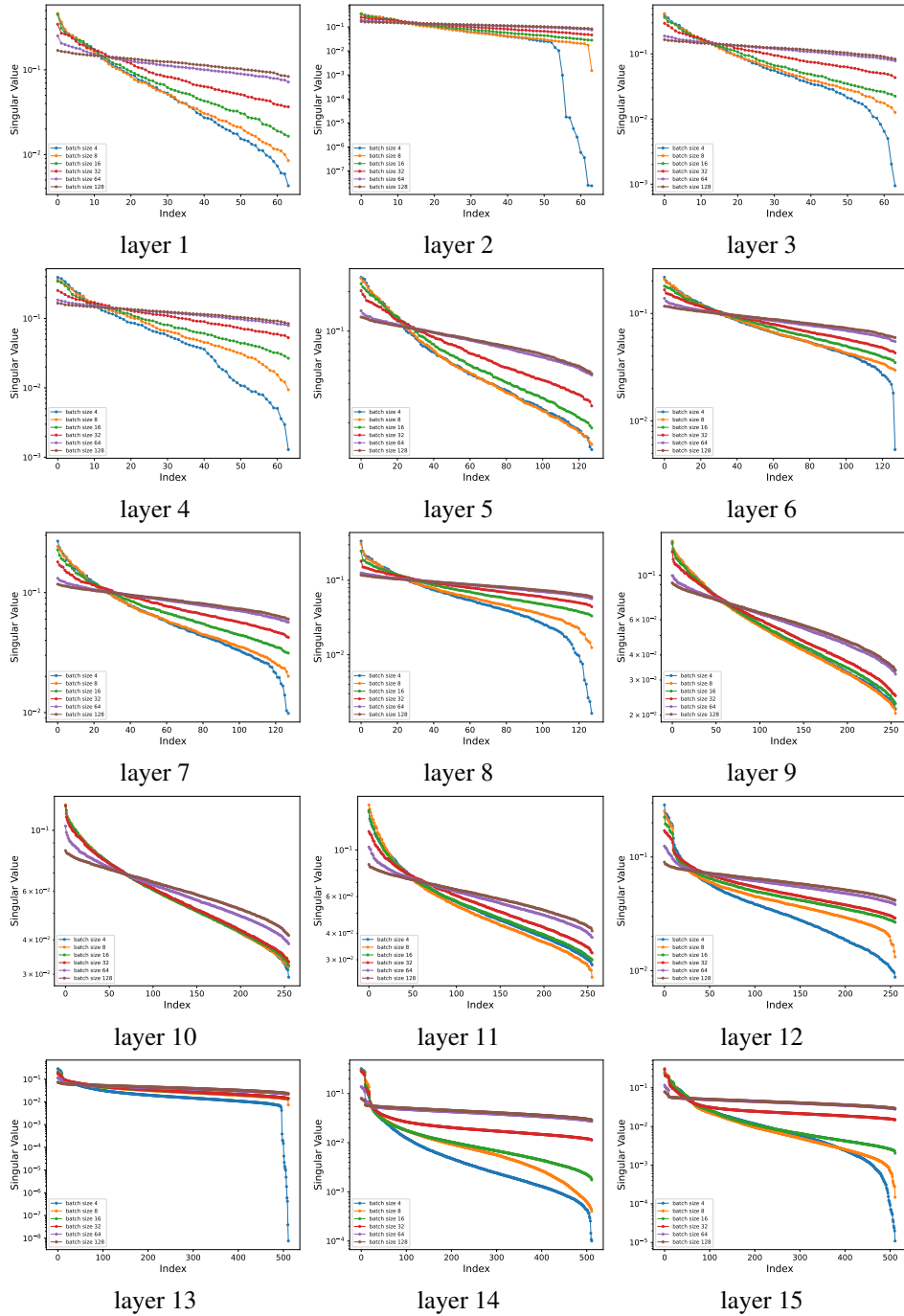


Figure 16: **Singular values of the weight matrices of ResNet-18 trained on CIFAR10 when varying B .** Each model was trained with $\mu = 5e-3$ and $\lambda = 6e-3$. Each plot reports the singular values of a given layer (see Fig. 3(b) in the main text for the averaged ranks and accuracy rates).

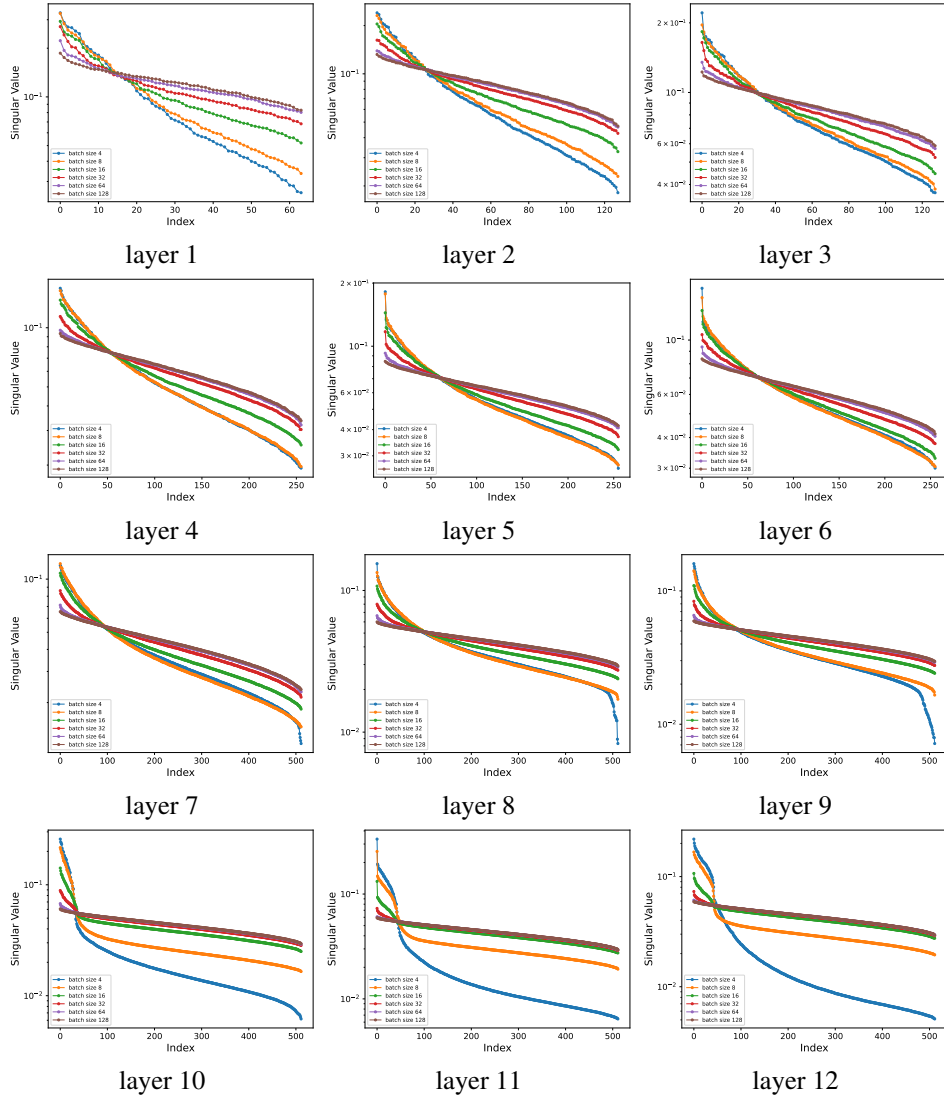


Figure 17: Singular values of the weight matrices of VGG-16 trained on CIFAR10 when varying B . Each model was trained with $\mu = 1e-2$ and $\lambda = 4e-4$. Each plot reports the singular values of a given layer (see Fig. 12(c) for the averaged ranks and accuracy rates).